Journal of Zoology

Postnatal remodeling of the laryngeal airway removes body size-dependency of spectral features for ultrasonic whistling in laboratory mice

Journal:	*Journal of Zoology*
Manuscript ID	JZO-07-21-OM-186.R2
Manuscript Type:	Original Manuscript
Date Submitted by the Author:	n/a
Complete List of Authors:	Darwaiz, Tarana; Midwestern University Pasch, Bret; Northern Arizona University Riede, Tobias
Keywords:	rodents, development, airway

Postnatal remodeling of the laryngeal airway removes body size-dependency of spectral features for ultrasonic whistling in laboratory mice

Tarana Darwaiz, Bret Pasch, Tobias Riede

Department of Physiology, College of Graduate Studies, Midwestern University Glendale, AZ, USA

Keywords: vocal production; mammals; geometric morphometrics; ultrasonic vocalization

Abstract

In many mammals, spectral properties of acoustic signals scale with body size within and among species. In rodents, however, despite drastic changes in body size, fundamental frequency (F0) range of ultrasonic whistles produced for social communication remain relatively uniform from birth to adulthood. Such divergent patterns may be due to a novel sound production mechanism unique to rodents involving an intralaryngeal midline pocket termed the ventral pouch. In this study, we analyzed the postnatal shape and size of the laryngeal airway in CD1 mice over ontogeny to better understand the association between ventral pouch geometry and F0 of ultrasonic whistles. Ventral pouch volume (0.06±0.01 mm^3) did not differ between pups and 1-year-old adults despite extensive shape-inducing remodeling of the intralaryngeal musculature and connective tissue. In contrast, ventral pouch volume was 50% smaller in 2-year-old compared to 1-year-old mice. Thus, allometry of the laryngeal airway appears to explain spectral overlap between ultrasonic whistles of young, small mice and older, larger mice. The causal association between the reduction in vocal behavior and a seemingly shrinking ventral pouch in geriatric mice remains unclear. Together, these data inform our understanding of the postnatal development and remodeling of the intralaryngeal airway in *Mus musculus*.

Introduction

In many mammals, body size is often correlated with the fundamental frequencies (F0) of vocalizations (e.g., Tembrock 1996; Fletcher 2004; Gillooly and Ophir 2010, Riede and Brown 2013, Charlton and Reby 2016). However, anatomical or physiological innovations can overcome size constraints. For example, vocal fold length and tension determine F0 range (Titze et al. 2016), but the amount and organization of viscoelastic collagen and elastic fibers in the lamina propria of vocal folds permits expansion of the spectral range beyond the boundaries defined by size (Titze et al. 2016). In humans, both vocal fold length and viscoelastic properties change with age (e.g., Kahane 1987; Hirano et al. 2000; Filho et al. 2003; Abdelkafy et al. 2007), leading to (sometimes large) age (e.g., Heylen et al.1998; Siupsinskiene, Lycke 2011) and sex differences (e.g., Hammond et al. 1998, Titze 1989) in F0 ranges. Similarly, vocal tract length determines resonance frequencies. However, some species can modify resonance spectral range into higher or lower regions through dynamic modulation of vocal tract length via a flexible larynx position (e.g., Reby, McComb 2003; Nishimura et al. 2003) or the ability to protrude or retract lips (Hauser, Ybarra 1994). Both mechanisms (vocal fold design and vocal tract flexibility) provide adaptations to escape the size-typical spectral range to produce vocal signals with higher or lower frequencies.

Rodents produce a rich repertoire of high-frequency communication signals in a variety of social contexts (e.g., Shelley, Blumstein 2005; Brudzynski 2018; Dent et al. 2018). For example, pup isolation vocalizations used to induce maternal care are ubiquitous among rodents (Lingle et al. 2012). In addition, many rodents produce vocalizations as adults to mediate a variety of social interactions, including mate acquisition (Fernandez et al. 2021). Surprisingly, although spectral features of vocal repertoires differ at various life stages (e.g., Grimsley et al.

2013; Riede et al. 2015; Zaytseva et al. 2019; Yurlova et al. 2020), the F0 ranges of certain high-frequency vocalizations (aka 'ultrasonic vocalizations', USVs) overlap between small pups and large adults (e.g., Liu et al. 2003; Grimsley et al. 2011; Yurlova et al. 2020). The phenomenon is also known in other rodents (e.g., Matrosova et al. 2007). In lab mice (*Mus musculus*), for example, temporal and spectral features of ultrasonic whistles can reliably differentiate pup and adult vocalizations. However, the F0 *range* used by pups and adults appears remarkably similar (e.g., Liu et al. 2003). Such a pattern stands in stark contrast with allometric relationships that typify vertebrate vocalizations produced by airflow-induced vocal fold vibration. In contrast to the clear dependency of F0 range on size and viscoelastic properties of vocal folds , the factors underlying F0 regulation in rodent whistle production are incompletely understood. A more detailed description of the anatomy of the rodent vocal organ and its airway is needed to inform our understanding of the mechanisms that permit such atypical non-allometry of vocal frequencies.

The larynx and its airway are part of the upper respiratory tract. Control of the larynx plays a role in breathing, swallowing, and vocalization. Understanding the function of anatomical structures underlying behavioral performance requires characterization of such structures over ontogeny. In humans, for example, the laryngeal cartilaginous framework (Kahane 1982; Eckel et al. 1999), the vocal fold tissue, (Ishii et al. 2000; Hartnick et al. 2005; Lungova et al. 2015) and the intralaryngeal airway experience shape changes and remodeling during ontogeny (Wheeler et al. 2009) with consequences for speech, breathing, and swallowing (Bosma 1985; Stevenson, Allaire 1991). In nonhuman species, ontogenetic changes in vocal organ form, shape, and mechanical properties contribute to functional changes in vocal patterns (e.g., tungara frog: Guerra et al. 2014; American alligator: Riede et al. 2011; zebra finch: Wade

et al. 2002; Veney & Wade 2005; Goitred gazelle: Efremova et al. 2016; North American elk: Frey, Riede 2013; nonhuman primates: Zhang et al. 2019). With the increasing accessibility to emerging imaging technologies (e.g micro-CT), the mouse model (*Mus musculus*) offers a more tractable model to explore the form-function relationship in detail.

In rodents, laryngeal sound is either produced by airflow induced vocal fold vibrations or an aerodynamic whistle mechanism (Roberts 1975; Pasch et al. 2017). Many high-fundamental frequency vocalizations produced by *Mus* are generated via the latter mechanism. Riede et al. (2017) proposed an edgetone mechanism model, which in contrast to an alternative jet mechanism model (Mahrt et al. 2016), predicts a strong relationship between ventral pouch size and vocal frequency. Briefly, spectral properties of whistles produced by an edgetone mechanism depend on airflow velocity and the geometry of the sound source (Coleman 1973; Fletcher 1973). In mice, whistles are produced inside the larynx when an expiratory glottal airflow interacts with rigid structures behind (i.e., rostral from) the vocal folds. Production of high-frequency whistles is dependent on the intactness of both the intra-laryngeal supraglottal ventral pouch and the alar cartilage located at the entrance of the ventral pouch (Riede et al. 2017). Damage to either the ventral pouch and/or the alar cartilage compromises a rodent's ability to produce ultrasonic vocalizations (Riede et al. 2017). The geometry of the ventral pouch is controlled through intrinsic laryngeal muscle activity, whereby contraction of a portion of the thyroarytenoid muscle moves the alar cartilage closer to the glottis (Riede 2013). However, this movement is limited and therefore the intralaryngeal airway, including ventral pouch morphology (i.e., size and shape), likely contributes to acoustic variation. Such a difference in the sound production mechanism of whistles may explain the size-independence of vocal frequencies.

In this study, we investigated size and shape changes of the laryngeal airway. Larynx size scales allometrically with body size and the laryngeal cartilaginous framework experiences shape changes throughout life (Riede et al. 2020). However, because fundamental frequencies of *Mus* vocalizations overlap between pups and larger adults, we hypothesized that there would be little change in size to the laryngeal airway underlying vocal production.

Methods

Study sample

Postnatal development of ventral pouch size and shape was quantified in 30 mice (*Mus musculus*, CD 1 strain, colony maintained at MWU). Animals were housed in same sex groups of 3 to 5 animals in standard rodent cages (33cm long x 18cm wide x 14cm deep) on a 12:12 h light/dark cycle. Rodent chow and water were available ad libitum. Animals (3/sex) were raised to 5 age classes (postnatal days 2, 21, 90, 365 and 755). Adult animals (365 and 755 days) were temporarily used for breeding, and thus experienced hormonal changes that could affect laryngeal shape (e.g., Saez, Martin 1976; Aufdemorte et al. 1983).

Following euthanasia with ketamine and xylazine, mice were transcardially perfused with lactated Ringer solution, and tissues were fixed with 10% buffered formalin phosphate (SF100-4; Fisher Scientific). Larynx tissue was then dissected, stained, and imaged using a microCT scanner (Skyscan 1172; Bruker-microCT, Kontich, Belgium) at 5 micrometer resolution. Further details can be found in Riede et al. (2020). Derived three-dimensional surfaces in STL format of the intralaryngeal airway and thyroid cartilages are available on Morphobank (O'Leary and Kaufman 2012) (project P4018).

Morphometric Analysis

Ventral pouch size was estimated by linear measures and volume estimates. Three linear measures were: (a) distance between glottal and alar edge ("CC"), (b) largest latero-lateral distance ("LL"), and (c) the distance between the most ventral point and a line described by distance CC ("VD") (Figure 1). The volume was estimated using the 3D model surface. The STL files of the 30 ventral pouches were uploaded to FIJI-ImageJ (Schindelin et al. 2012). The 3D viewer plugin facilitates visualization and volume calculation. The size of the thyroid cartilage was estimated using the thyroid cartilage bounding box volume. Bounding box refers to the minimum enclosing box for the set of points comprising the 3D rendition of a structure present in STL format. The ratio between the bounding box volume and the ventral pouch volume was used as an estimate for ventral pouch shape and size change with age.

Three-dimensional geometric morphometrics was used to describe shape of the ventral pouch. We established a set of 5 fixed and 50 semi-(surface) landmarks using the *geomorph* package (Adams et al. 2017) in R 3.4.4 (R Core Team 2015). The 5 fixed landmarks were placed interactively in mid-sagittal position on the alar edge, the glottal edge, on the most left and right lateral points and on the most ventral point of the ventral pouch. The landmark coordinate data were then superimposed using generalized Procrustes analysis (GPA) for each set of landmarks analyzed (Gower, 1975; Rohlf and Slice 1990). This produces a set of transformed coordinates that reflect shape differences among cartilages independent of scaling. Then a principal component analysis was done to derive shape axes. Those shape axes (principal components) help to convert variation in shape into a set of linearly uncorrelated variables.

Acoustic analysis

For three of five age classes (PND 2, 90, 365), ultrasonic whistles were successfully recorded. Recording attempts in weanlings (PND 21) and in geriatric mice (PND 755) were unsuccessful. Pup vocal behavior was triggered by a 1 minute separation of the pup from the litter. Vocalizations in 90 and 365 day-old animals was induced by placing the animal into a separate cage and adding bedding of the opposite sex. Further details on sound recording can be found in Riede et al. (2020).

We analyzed 1008 syllables from six pups, 104 syllables from three young adults (PND 90) and 287 syllables from five adult mice (PND 365). Syllable types were not assigned because all syllables were ultrasonic vocalizations produced by the same whistle mechanism. Fundamental frequency was quantified every 30 ms using the pitch tracking tool in PRAAT (PRAAT software, v. 5.2.12). Visual inspection confirmed that frequency tracking was successful. The frequency was extracted every 5 ms and placed in 500Hz bins. Center frequency was determined as the frequency bin in which the median of the data sample was located. Minimum and maximum fundamental frequency represented the lowest and the highest value in the histogram.

Statistical Analysis

Univariate analysis was performed to assess ventral pouch growth. An analysis of variance (ANOVA) was used to test for age differences in three linear ventral pouch distances, ventral pouch volume, and two shape axes (principal components). Scaling relationships of various dimensions on body mass were analyzed using Pearson correlation coefficients. We performed a Kolmogorov-Smirnov test on the distribution of fundamental frequencies between the three age classes to test for statistical significance.

Results

Figure 2 illustrates ventral views and midsagittal sections of 3D renditions of the thyroid cartilage and the laryngeal airway. The airway is shown in two colors with the main airway in yellow and the ventral pouch in blue. Figure 3 provides three different views of the laryngeal airway of all 30 CD1 mice. Table 1 provides a summary of linear and volumetric measurements in this mouse sample. The ventral pouch is relatively large and shaped like a sphere in 2-day old pups but appears flattened, disk-shaped, and relatively smaller in older individuals. All three linear dimensions were different among the five age classes (ANOVA, LL: $F_{4,25}$=8.82, p<0.001; VD: $F_{4,25}$= 4.42, p<0.01; CC: $F_{4,25}$=16.4, p<0.001) (Table 1). Two measures (LL and VD) showed no change in size during the first year (Pearson correlation, LL: $r = 0.25$, $p = 0.25$; VD: $r = 0.26$, $p = 0.22$) (Figure 4 A and B). In other words, we found no increase in size associated with overall body size. The CC distance increased by a factor of 1.9 from pups to one-year-old adults (Pearson correlation, $r = 0.83$, $p < 0.01$) (Figure 4C). All three distances were smaller in 2-year old than in 1-year old mice (t-test, LL: $t_{1,10} = 3.98$, $p < 0.01$; VD: $t_{1,10} = 4.0$, $p < 0.01$; CC: $t_{1,10} = 3.07$, $p < 0.01$) (Table 1; Figure 4).

Laryngeal size estimated by the bounding box differed among five age classes ($F_{4,25}$=110.7, p<0.001) and increased with age (Pearson correlation, $r = 0.84$, $p < 0.001$) (Figure 3D). The size of the ventral pouch did not change with age (Table 1) (Figure 4E). Ventral pouch volume was not significantly different between the first four age classes ($F_{3,23}$=1.0, p = 0.41). Ventral pouch volume was smaller in two-year old than in one-year old mice (t-test, $t_{1,10} = 3.07$, $p < 0.01$). The ratio between thyroid cartilage bounding box volume and ventral pouch volume decreased from about 1.7±0.4% in pups to 0.27±0.08% in old adults ($F_{4,25}$=53.1, p < 0.001; $r = -0.55$, $p < 0.01$)

(Figure 4F). Data suggest that ventral pouch volume is maintained throughout most of the postnatal development despite the increase in size of the larynx and its lumen. For all six laryngeal variables listed in Table 1, the differences between males and females were not statistically significant (ANOVA, $p>0.05$).

The ventral pouch changed in shape from sphere-like to disk-shaped (Figures 2 and 3). Next, we quantified ventral pouch shape using surface landmarks. The first and second shape axes described 56% and 15%, of the variation, respectively. The first but not the second shape axis differentiated among the 5 age classes (ANOVA, PC1: $F_{4,25}=32.4$, $p<0.001$; PC2: $F_{4,25}= 2.21$, $p=0.09$) and all plots that included the first axis similarly differentiated the five age classes (Figure 4G and H).

Figure 5 illustrates the extent of the intra-laryngeal airway remodeling. Virtual coronal sections through the larynx organs show that the ventral pouch airway fills the entire lumen between the two thyroid cartilage lamina in pups. In adults, the lumen within the thyroid cartilage is filled with airway and soft connective tissue (Figure 5).

Finally, we investigated the association between body size, ventral pouch size and spectral properties of high frequency whistles. Importantly, all three age classes produced sound across the entire range between 30 and 90 kHz. Figure 6 A illustrates spectrographic images of 8 inverted-U shaped syllables produced by a female pup. Fundamental frequency was tracked every 5 ms. The overlaid tracking result is shown in Figure 6B. Figure 6C illustrates the extracted fundamental frequency measurements. The most prominent frequency in those 8 syllables was 60 kHz, the center frequency was 50.8kHz, minimum frequency was 37.7 and maximum frequency was 64.0 kHz (Figure 6C).

The frequency distribution of three *Mus* age classes are shown in Figure 6D. The frequency distribution between pups and 90-day old mice (Kolmogorov-Smirnov, Z=0.96; P>0.05), and between pups and 365-day old mice did not differ (Kolmogorov-Smirnov, Z=0.96; P>0.05). The distribution was different between 90-day old and 365-day old mice (Kolmogorov-Smirnov, Z=1.54; P<0.05). Neither body mass nor ventral pouch size explain center (Pearson correlation, r = -0.43 and -0.32, $p > 0.05$), minimum (r = -0.90 and -0.94, $p > 0.05$) or maximum fundamental frequency (r = 0.10 and -0.76, $p > 0.05$) (Figure 6D, E).

Discussion

The results of our experiments suggest that shape and size changes of laryngeal cartilages (Riede et al. 2020) are accompanied by intralaryngeal airway changes. Specifically, although the ventral pouch maintains a similar size for the first year despite a massive increase in body mass and larynx size, it shrinks by approximately 50% between PND 365 and PND 755. Ventral pouch shape in pups and weanlings was also different from older animals. Both the remodeling of the laryngeal cartilaginous framework (Riede et al. 2020), the intralaryngeal soft tissue (Tateya et al. 2006) and the laryngeal airway (this study) inform our understanding of the functional morphology of the rodent larynx. We explore the implications of our findings for understanding high frequency whistle production in rodents and discuss factors that determine upper airway form and function.

Implications for rodent aerodynamic whistle production

The edge-tone model of whistle production (Riede et al. 2017) predicts that ventral pouch size corresponds to vocal frequencies. This prediction is supported by large ventral pouch sizes in *Baiomys* (Riede, Pasch 2020) and *Scotinomys* (Smith et al. 2021), both species that produce unusually low-pitched ultrasonic whistles. Our findings herein further support predictions of the edge-tone hypothesis; young and old mice had similar sized ventral pouch volumes and overlapped in their spectral ranges. The absence of a quantifiable ventral pouch volume increase during the first year is consistent with the overlap in spectral ranges between pups and older *Mus musculus* (Grimsley et al. 2011) and other rodents (see Wiaderkiewicz et al. 2013; Hulsmann et al. 2019; *Scotinomys*: Campbell et al. 2014). Although the functional significance of such overlap is unclear (e.g. see Matrosova et al. 2007), active control of intralaryngeal airway geometry by intrinsic muscles likely helps maintain a large spectral range (Riede 2011, 2013). In our study, each of the three age classes achieved a considerable fundamental frequency range (Figure 6).

Validation of this hypothesis would benefit from comparisons of vocalizations from older mice with reduced vocal pouch sizes. However, vocal activity declines in aging mice and we were unable to record vocalizations in geriatric animals. In males, vocal decline has been ascribed to hormonal changes and pheromonal processing (e.g., Kanno, Kikusui 2018; Nyby 2010). Our study indicates that morphological changes of the vocal organ and the upper airway may also play a role. Further experimental manipulation of the laryngeal airway could provide insight into whether morphological airway remodeling precedes or follows the behavioral change.

Factors that determine phenotypic variation of larynx and upper airway

Postnatal laryngeal airway remodeling is well-known in humans and is clinically relevant (Wheeler et al. 2009). The intralaryngeal lumen develops from a conical shape to a more cylindrical tube (Figure 7). In CD1 mice, airway remodeling resembles this change from a wide intralaryngeal space narrowing caudally to a more uniform tubular lumen. The airway remodeling is in part a consequence of the shape changes of the laryngeal cartilaginous framework (e.g. the thyroid cartilage becomes wider in the latero-lateral dimension; Riede et al. 2020). Furthermore, soft tissue (Figure 5) accumulates in the laryngeal lumen being part of the ventral pouch's boundary.

The genetic and environmental factors determining the remodeling are likely complex. The larynx is of mixed embryological origin (Tabler et al. 2017; Heude et al. 2018). Thyroid cartilage originates from neural crest tissue and cricoid cartilage, arytenoid cartilages, epiglottis, musculature and soft connective tissue (like vocal ligament) from mesoderm. The laryngeal airway including the ventral pouch is therefore dependent on the development of both mesoderm and neural crest tissue (Tabler et al. 2017; Heude et al. 2018).

Environmental risk factors such as age and obesity may affect motor function and neurochemical control of the upper airway with consequences for airway patency (e.g., Brennick et al. 2009; Polotsky et al. 2011; Takahasi et al. 2020; Voituron et al. 2010). Airway remodeling has been reported for obese rats and mice (Nakano *et al.* 2001, Ogasa *et al.* 2004; O'Donnell *et al.* 1999; Polotsky *et al.* 2001, 2004). Those studies have focused on the pharyngeal area. The current study demonstrates that the intralaryngeal airway is also remodeled throughout life of a mouse. The mechanism by which risk factors affect this process remains to be seen. The exploration of those factors seems worthwhile because the larynx has not only been implicated in the etiology of sleep apnea and other problems associated with upper airway patency (e.g.,

Dedhia et al. 2014; Roy et al. 2021) but its evolvability remains speculative (Kingsley et al. 2018). The current study illustrates also a methodological approach to quantify shape changes in the upper respiratory airway.

Caveats

We found considerable among-individual variation in laryngeal size and shape within age classes (Table 1). The variation within each class remains unexplained, but tissue preparation may have contributed. The current study used fixed tissue to quantify laryngeal airway dimensions. Future studies should include laryngeal airway analyses *in vivo*. However, even if one takes a fixation-related shrinkage into account, any deformation is countered by the cartilage enforced structure of the larynx and it should apply equally to all age classes. However, we expect this effect to be small on the overall results for two reasons. First, the constancy of the ventral pouch volume is associated with massive tissue remodeling inside the larynx (Figure 5) in the first year of life. Second, the thyroid cartilage experiences shape changes between PND 365 and 755 (Figure 5) which is associated with the shrinkage of the ventral pouch at old age.

Finally, many of the 1-year old and 2-year old adult mice were retired breeders, i.e. they have gone through mating and pregnancy related hormonal changes. Since estrogen, progesterone, and testosterone effect cartilage remodeling (e.g., DaSilva et al. 1993; Richette et al. 2003; Johnston et al. 2021; Montoya-Sanhueza et al. 2021), formal assessment it remains to be seen how large this effect is on the post-puberty larynx.

Conclusion

Our findings herein suggest an alternative mechanism to remove constraints on the allometric relationships between size and spectral range. The size of a musical instrument is in many cases a good predictor of its spectral range (i.e., fundamental frequency and resonant frequency range). For ultrasonic whistling in rodents, it seems that remodeling of the laryngeal airway and the evolution of a novel structure (ventral pouch) enables extension of the spectral range of vocal signals. Together with how the instrument is played, i.e. the neural control which coordinates movements of the vocal organ (e.g., Nieder, Mooney 2020; Fernandez-Vargas et al. 2021), the constancy of ventral pouch lumen provides a compelling example for size-independency of the spectral range.

The constraints responsible for maintaining laryngeal airway features could be two-fold. First, the functional morphology required to produce whistles seems to depend on the integrity of the ventral pouch and its active control of shape and lumen (Riede et al. 2017). Second, changes in laryngeal airway likely also affect normal respiratory airflow patterns with subsequent consequences for gas exchange and penetrance of pathogens (e.g., Sagartz et al. 1992; Renne et al. 1992). The reasons for the static nature of the ventral pouch remain to be further explored.

References

Abdelkafy WM, Smith JQ, Henriquez OA, et al. Age-related changes in the murine larynx: initial validation of a mouse model. *Ann Otol Rhinol Laryngol* 2007; 116: 618– 622.

Adams, D. C., Collyer, M. L., Kaliontzopoulou, A., and Sherratt, E. (2017). Geomorph: Software for geometric morphometric analyses. R package version 3.0.5. (https://cran.r-project.org/package=geomorph.)

Aufdemorte, TB, Sheridan, PJ, Holt, GR 1983. Autoradiographic evidence of sex steroid receptors in the laryngeal tissues of the baboon (*Papio cynocephalus*). Laryngoscope; 93: 1607–11.

Bosma, J.F. (1985). Postnatal ontogeny of performance of the pharynx, larynx, and mouth. *American Review of Respiratory Diseases*. 131, S10–S15.

Brennick, MJ , Pack, AI , Ko, K , Kim, E , Pickup, S , Maislin, G , Schwab, RJ. (2009). Altered upper airway and soft tissue structures in the New Zealand Obese mouse. *Am J Respir Crit Care Med 179*, 158–169.

Brudzynski, S.M. (2018). Handbook of Ultrasonic Vocalization. A Window into the Emotional Brain. Volume 25; Academic Press.

Campbell, P., Pasch, B., Warren, A.L., Phelps, S.M. (2014). Vocal ontogeny in neotropical singing mice (*Scotinomys*). *PloS One* 9, e113628

Charlton, B. D. & Reby, D. (2016). The evolution of acoustic size exaggeration in terrestrial mammals. *Nature Communications* 7, 12739.

Coltman, J. W. (1976). Jet drive mechanisms in edge tones and organ pipes. *The Journal of the Acoustical Society of America*, *60*(3), 725–733.

Da Silva, J.A., Larbre, J.P., Spector, T.D., Perry, L.A., Scott, D.L., Willoughby, D.A. (1993). Protective effect of androgens against inflammation induced cartilage degradation in male rodents. *Annals of the Rheumatic Diseases* 52, 285-291.

Dedhia, R.C., Rosen, C.A., Soose, R.J. (2013). What is the role of the larynx in adult obstructive sleep apnea. *The Laryngoscope* 124, 1029-1034.

Dent, M.L., Fay, R.R., Popper, A.N. (2018). Rodent Bioacoustics. *Springer Handbook of Auditory Research* book series (SHAR, volume 67).

Eckel, H.E., Koebke, J., Sittel, C., Sprinzl, G.M., Potoschnig, C., Stennert, E. (1999). Morphology of the human larynx during the first five years of life studied on whole organ serial sections. *Annals of Otology, Rhinology & Laryngology* 108, 232–238.

Efremova, K.O., Frey, R., Volodin, I.A., Fritsch, G., Soldatova, N.V., Volodina, E.V. (2016). The postnatal ontogeny of the sexually dimorphic vocal apparatus in goitred gazelles (*Gazella subgutturosa*). *J Morphology* 277, 826-844.

Fernandez-Vargas, M., Riede, T., Pasch, B. (2021). Mechanisms and constraints underlying acoustic variation in rodents: emerging themes and future directions. *Animal Behavior*, in press.

Filho JAX, Tsuji DH, Nascimento PH, Sennes LU. Histologic changes in human vocal folds correlated with aging: a histomorphometric study. *Ann Otol rhinol Laryngol* 2003; 112: 894–899.

Fletcher, N. H. (1979). Air Flow and Sound Generation in Musical Wind Instruments. *Annual Review of Fluid Mechanics*, 11, 123–146.

Fletcher, N. H. (2004). A simple frequency-scaling rule for animal communication. *J. Acoust. Soc. Amer*. 115, 2334-2338.

Frey, R., Riede, T. (2013). The anatomy of vocal divergence in North American elk and European red deer. *J. Morphology* 274*,* 307-319.

Gillooly, J.F., Ophir, A.G. (2010). The energetic basis of acoustic communication. *Proceedings of the Royal Society B* 277, 1325–1331.

Gower, J.C. (1975). Generalized procrustes analysis. *Psychometrika* 40, 33-51.

Grimsley, J.M.S., Monaghan, J.J.M., Wenstrup, J.J. (2011). Development of Social Vocalizations in Mice. *PLoS One* 6, e17460.

Grimsley, J., Gadziola, M., Wenstrup, J. (2013). Automated classification of mouse pup isolation syllables: from cluster analysis to an Excel-based "mouse pup syllable classification calculator". *Front. Behav. Neurosci.* 6, 10.3389.

Guerra, M.J., Ryan, M.J., Cannatella, D.C. (2014). Ontogeny of sexual dimorphism in the larynx of the Túngara Frog, *Physalaemus pustulosus. Copeia* 2014, 123-129.

Hammond TH, Gray SD, Bulter J, Zhou R, Hammond E. Age- and gender-related elastin distribution changes in human vocal fold. *Otolaryngol Head Neck Surg* 1998; 119: 314– 322.

Hartnick, C.J., Rehbar, R., Prasad, V. (2005). Development and maturation of the pediatric human vocal fold lamina propria. *The Laryngoscope* 115, 4-15.

Hauser, M.D., Ybarra, M.S. (1994). The role of lip configuration in monkey vocalizations: experiments using xylocaine as a nerve block. *Brain and language* 46, 232-244.

Heude, E., Tesarova, M., Sefton, E. M., Jullian, E., Adachi, N., Grimaldi, A., Zikmund, T., Kaiser, J., Kardon, G., Kelly, R. G., Tajbakhsh, S. (2018). Unique morphogenetic signatures define mammalian neck muscles and associated connective tissues. *eLife*, 7, e40179.

Heylen, L., Wuyts, F.L., Mertens, F., Bodt, M.D., Pattyn, J., Croux, C. and Heyning, P.H.V.D., 1998. Evaluation of the vocal performance of children using a voice range profile index. *Journal of Speech, Language, and Hearing Research*, *41*(2), pp.232-238.

Hirano M, Sato K, Nakashima T. Fibroblasts in geriatric vocal fold mucosa. *Acta Otolaryngol* 2000; 120: 336– 340.

Hülsmann, S., Oke, Y., Mesuret, G., Latal, A. T., Fortuna, M. G., Niebert, M. (2019). The postnatal development of ultrasonic vocalization-associated breathing is altered in glycine transporter 2-deficient mice. *J. Physiol.* 597, 173–191.

Ishii, K., Yamashita, K., Akita, M., Hirose, H. (2000). Age-related development of the arrangement of connective tissue fibers in the lamina propria of the human vocal fold. *Ann Otol Rhinol Laryngol* 109, 1055-1064.

Johnston, R.A., Vullioud, P., Thorley, J., Kirveslahti, H., Shen, L., Mukherjee, S., Karner, C.M., Clutten-Brock, T., Tung, J. (2021). Morphological and genomic shifts in mole-rat 'queens' increase fecundity but reduce skeletal integrity. *eLife* 10, e65760.

Kahane, J. C. (1982) Growth of the human prepubertal and pubertal larynx. *Journal of Speech and Hearing Research* 25, 446-455.

Kahane JC. (1987) Connective tissue changes in the larynx and their effects on voice. *J Voice*; 1: 27– 30

Kanno K, Kikusui T. (2018). Effect of sociosexual experience and aging on number of courtship ultrasonic vocalizations in male mice. *Zoolog Sci*. 35, 208–214.

Kingsley, E.P., Eliason, C.M., Riede, T., Li, Z., Hiscock, T.W., Farnsworth, M., Thomson, S.L., Goller, F., Tabin, C.J., Clarke, J.A. (2018). Identity and novelty in the avian syrinx. *PNAS* 115, 10209–10217.

Lingle, S., Wyman, M.T., Kotrba, R., Teichroeb, L.J., Romanow, C.A. (2012). What makes a cry a cry? A review of infant distress vocalizations. *Current Zoology* 58, 698-726.

Liu, R.C., Miller, K.D., Merzenich, M.M., Schreiner, C.E. (2003). Acoustic variability and distinguishability among mouse ultrasound vocalizations. *J Acoust Soc Am* 114, 3412–3422.

Lungova, V., Verheyden, J.M., Herriges, J., Sun, X., Thibeault, S.L. (2015). Ontogeny of the mouse vocal fold epithelium. *Developmental Biology* 399, 263-282.

Mahrt, E., Agarwal, A., Perkel, D., Portfors, C., Elemans, C.P. (2016). Mice produce ultrasonic vocalizations by intra-laryngeal planar impinging jets. *Curr. Biol*. 26, R880–R881.

Matrosova, V.A., Volodin, I.A., Volodina, E.V. (2007). Pups crying bass: vocal adaptation for avoidance of age-dependent predation risk in ground squirrels? *Behav Ecol Sociobiol* 62, 181–191.

Montoya-Sanhueza G, Bennett, N.C., Oosthuizen, M.K., Dengler-Crish, C.M., Chinsamy, A. (2021). Bone remodeling in the longest living rodent, the naked mole rat: Interelement variation and the effects of reproduction. *J. Anatomy* 239, 81-100.

Nakano, H., Magalang, U.J., Lee, S.D., Krasney, J.A., Farkas, G.A. (2001). Serotonergic modulation of ventilation and upper airway stability in obese Zucker rats. *Am J Respir Crit Care Med* 163, 1191–1197.

Nieder, A., Mooney, R. (2020). The neurobiology of innate, volitional and l earned vocalizations in mammals and birds. *Philos. Trans. R. Soc. Lond. B Biol. Sci.* 375, 20190054.

Nishimura, T., Mikami, A. Suzuki, J., Matsuzawa, T. (2003). Descent of the larynx in chimpanzee infants. *Proceedings of the National Academy of Sciences* 100, 6930–33.

Nyby, J.G. (2010). Adult house mouse (*Mus musculus*) ultrasonic calls: hormonal and pheromonal regulation. In: Brudzynski SM, editor. Handbook of Mammalian Vocalization—An Integrative Neuroscience Approach: Elsevier Academic Press. p. 303–310.

O'Donnell, C.P., Schaub, C.D., Haines, A.S., Berkowitz, D.E., Tankersley, C.G., Schwartz, A.R., Smith, P.L. (1999). Leptin prevents respiratory depression in obesity. *Am J Respir Crit Care Med* 159, 1477–1484.

Ogasa, T., Ray, A.D., Michlin, C.P., Farkas, G.A., Grant, B.J., Magalang, U.J. (2004). Systemic administration of serotonin 2A/2C agonist improves upper airway stability in Zucker rats. *Am J Respir Crit Care Med* 170, 804–810.

O'Leary, M.A., Kaufman, S.G. (2012). MorphoBank 3.0: Web application for morphological phylogenetics and taxonomy.

Pasch, B., Tokuda, I.T., and Riede, T. (2017). Grasshopper mice employ distinct vocal production mechanisms in different social contexts. *Proc. Roy. Soc. Lond. B,* 284, 20171158.

Polotsky, V.Y., Smaldone, M.C., Scharf, M.T., Li, J., Tankersley, C.G., Smith, P.L., Schwartz, A.R., O'Donnell, C.P. (2004). Impact of interrupted leptin pathways on ventilatory control. *J Appl Physiol* 96, 991–998.

Polotsky, V.Y., Wilson, J.A., Smaldone, M.C., Haines, A.S., Hurn, P.D., Tankersley, C.G., Smith, P.L., Schwartz, A.R., O'Donnell, C.P. (2001). Female gender exacerbates respiratory depression in leptin-deficient obesity. *Am J Respir Crit Care Med* 164, 1470–1475.

Polotsky, M., Elsayed-Ahmed, A.S., Pichard, L.E., Richardson, R.A., Smith, P.L., Schneider, H., Kirkness, J.P., Polotsky, V.Y., Schwartz, A.R. (2011). Effect of age and weight on upper airway function in a mouse model. *J Appl Physiol* 111, 696–703.

Reby, D., McComb, K. (2003). Anatomical constraints generate honesty: Acoustic cues to age and weight in the roars of red deer stags. *Animal Behaviour* 65, 519–30.

Renne, R.A., Gideon, K.M., Miller, R.A., Mellick, P.W., Grumbein, S.L. (1992). Histologic methods and interspecies variations in the laryngeal histology of F344/N rats and B6C3F1 mice. *Toxicol Pathol* 20, 44-51.

Richette, P.R., Corvol, M., Bardin, T. (2003). Estrogens, cartilage, and osteoarthritis. *Joint Bone Spine* 70, 257-262.

Riede, T. (2011). Subglottal pressure, tracheal airflow and intrinsic laryngeal muscle activity during rat ultrasound vocalization. *Journal of Neurophysiology* 106, 2580-2592.

Riede, T., Tokuda, I.T., Farmer, C.G. (2011). Subglottal pressure and fundamental frequency control in contact calls of juvenile *Alligator mississippiensis*. *Journal of Experimental Biology* 214, 3082-3095.

Riede, T. (2013). Call type specific motor patterns in rat ultrasound vocalization. *Journal of Experimental Zoology A* 319, 213–224.

Riede, T. (2018). Peripheral vocal motor dynamics and combinatory call complexity of ultrasonic vocal production in rats. In Handbook of Ultrasonic Vocalization, edited by Stefan M. Brudzynski; Elsevier series '*Handbook of Behavioral Neuroscience'*, Vol 25, pp. 45-60.

Riede, T., Zhao, Y., LeDoux, M.S. (2015). Vocal development in dystonic rats. *Physiological Reports* 3, e12350.

Riede, T., Borgard, H., Pasch, B. (2017). Laryngeal airway reconstruction indicates rodent ultrasonic vocalizations are produced by an edge tone mechanism. *Royal Society Open Science* 4, 170976.

Riede, T., Brown, C. (2013). Body size, vocal fold length and fundamental frequency - Implications for mammal vocal communication. *Nova Acta Leopoldina NF* 111 380: 1–20.

Riede, T., Coyne, M., Tafoya, B., Baab, K.L. (2020). Postnatal development of the mouse larynx – negative allometry, age-dependent shape changes, morphological integration and a size-dependent spectral feature. *J Speech Lang Hear Res*. 63, 2680-2694.

Roberts, L.H. (1975). The rodent ultrasound production mechanism. *Ultrasonics*, 13, 83–88.

Rohlf, F.J., Slice, D. (1990). Extension of the Procrustes method for the optimal superimposition of landmarks. *Systematic Zoology* 39, 40-59.

Roy, N., Merrill, R.M., Pierce, J., Sundar, K.M. (2021). Evidence of possible irritable larynx syndrome in obstructive sleep apnea: an epidemiologic approach. *J Voice* https://doi.org/10.1016/j.jvoice.2020.02.006

Saez, SJ, Martin, PM 1976. Androgen receptors in human pharyngo-laryngeal mucosa and pharyngo-laryngeal epithelium. J Steroid Biochem; 7: 919–21.

Sagartz, J.W., Madarasz, A.J., Forsell, M.A., Burger, G.T., Ayres, P.H., Coggins, C.R. (1992). Histological sectioning of the rodent larynx for inhalation toxicity testing. *Toxicol Pathol* 20, 118-121.

Schindelin, J., Arganda-Carreras, I., Frise, E. (2012) Fiji: an open-source platform for biological-image analysis. Nature methods 9, 676-682.

Shelley, E.L., Blumstein, D.T. (2005). The evolution of vocal alarm communication in rodents. *Behavioral Ecology* 16, 169–177.

Siupsinskiene, N. and Lycke, H., 2011. Effects of vocal training on singing and speaking voice characteristics in vocally healthy adults and children based on choral and nonchoral data. *Journal of voice*, *25*(4), pp.e177-e189.

Smith, S.K., Burkhard, T.T., Phelps, S.M. (2021). A comparative characterization of laryngeal anatomy 1086 in the singing mouse. *J Anatomy* 238, 308-320.

Stevenson, R.D., Allaire, J.H. (1991). The development of normal feeding and swallowing. *Pediatric Clinics of North America* 38, 1439–53

Tabler, J. M., Rigney, M. M., Berman, G. J., Gopalakrishnan, S., Heude, E., Al-Lami, H. A., Yannakoudakis, B. Z., Fitch, R. D., Carter, C., Vokes, S., Liu, K. J., Tajbakhsh, S., Egnor, S. E. R., & Wallingford, J. B. (2017). Cilia-mediated Hedgehog signaling controls form and function in the mammalian larynx. *elife*, 6, e19153.

Takahashi, T., Sakai, N., Iwasaki, T. (2020). Detailed evaluation of the upper airway in the Dp(16)1Yey mouse model of Down syndrome. *Sci Rep* 10, 21323.

Tateya T, Tateya I, Munoz-del-Rio A, Bless DM 2006. Postnatal development of rat vocal folds. *Annals of Otology, Rhinology & Laryngology* 115, 215-224.

Tembrock, G. (1996). Akustische Kommunikation bei Säugetieren. Darmstadt, Germany: Wissenschaftliche Buchgesellschaft.

Titze, I.R., 1989. Physiologic and acoustic differences between male and female voices. *The Journal of the Acoustical Society of America*, *85*(4), pp.1699-1707.

Titze, I., Riede, T., Mau, T. (2016). Predicting Achievable fundamental frequency ranges in vocalization across species. *PLoS Comput. Biol.* 12, e1004907.

Veney, S.L., Wade, J. (2005). Post-hatching syrinx development in the zebra finch: an analysis of androgen receptor, aromatase, estrogen receptor α and estrogen receptor β mRNAs. *Journal of Comparative Physiology A* 191, 97-104.

Voituron, N., Clément, M., Dutschmann, M., Hilaire, G. (2020). Physiological definition of upper airway obstructions in mouse model for Rett syndrome. *Respiratory Physiology & Neurobiology* 173, 146-156.

Volodin, I.A., Zaytseva, A.S., Ilchenko, O.G., Volodina, E.V. (2015). Small mammals ignore common rules: A comparison of vocal repertoires and the acoustics between pup and adult Piebald shrews *Diplomesodon pulchellum*. *Ethology* 121, 103-115.

Wade, J., Buhlman, L., Swender, D. (2002). Post-hatching hormonal modulation of a sexually dimorphic neuromuscular system controlling song in zebra finches. *Brain research* 929, 191-201.

Wheeler, M., Cote, C.J., Todres, I.D. (2009). The Pediatric Airway. In Cote CJ, Lerman J, Todres ID *et al. eds.* A Practice of Anaesthesia for Infants and Children, 4th ed., Philadelphia, PA: Saunders Elsevier, pp. 237–273.

Wiaderkiewicz, J., Głowacka, M., Grabowska, M., Barski, J.J. (2013). Ultrasonic vocalizations (USV) in the three standard laboratory mouse strains: Developmental analysis. *Acta Neurobiol Exp*. 73, 557–563.

Yurlova, D.D., Volodin, I.A., Ilchenko, O.G., Volodina, E.V. (2020). Rapid development of mature vocal patterns of ultrasonic calls in a fast-growing rodent, the yellow steppe lemming (*Eolagurus luteus*). *PLoS ONE* 15, e0228892.

Zaytseva, A.S., Volodin, I.A., Ilchenko, O.G., Volodina, E.V. (2019). Ultrasonic vocalization of pup and adult fat-tailed gerbils (*Pachyuromys duprasi*). *PLoS ONE* 14, e0219749.

Zhang, Y.S., Takahashi, D.Y., Liao, D.A., Ghazanfar, A.A., Elemans, C.P.H. (2019). Vocal state change through laryngeal development. *Nature communications* 10, 1-12.

Acknowledgement: Financial support for this work provided by the National Science Foundation IOS # 1754332 and by the NIDDK Mouse Metabolic Phenotyping Centers (RRID:SCR_008997, MMPC, www.mmpc.org) under the MICROMouse Funding Program, grants DK076169.

Data availability: Derived 3D surfaces of airways have been archived at Morphobank, project # P4018.

Author contributions: TD, BP and TR conceived and designed the study. TD lead the data analysis. BP, TR conducted the statistical analyses and drafted the manuscript. All authors provided edits on the drafts of the manuscript and gave the final approval for publication.

Table 1: Averages and standard deviations of linear measures and volumes of the ventral pouch as well as a volume ratio in five age classes of CD 1 mice. Six animals (3 per sex) were analyzed in each age class.

Age class		Body mass (g)	LL (µm)	VD (µm)	CC (µm)	VP volume (mm^3)	B-Box volume (mm^3)	B-Box/VP ratio (%)
PND 2	M:	4.0±1.7	681±13.0	311±83.1	493±14.1	0.0609±0.007	3.7±1.7	1.8±0.5
	F:	5.0±1.7	689±14.7	326±45.0	519±21.4	0.0706±0.007	4.6±1.0	1.6±0.3
PND 21	M:	13.3±0.6	680±96.6	346±58.4	565±39.1	0.0721±0.015	10.7±0.7	0.7±0.2
	F:	13.3±2.3	690±72.3	331±79.4	575±23.0	0.0674±0.007	9.1±0.9	0.7±0.1
PND 90	M:	29.7±5.0	547±40.6	316±68.8	676±45.4	0.0484±0.011	16.7±1.5	0.3±0.05
	F:	40.3±2.8	615±135.5	332±17.8	644±99.3	0.0626±0.030	18.0±3.2	0.4±0.2
PND 365	M:	60.3±4.0	694±39.2	308.7±6.8	725±60.9	0.0656±0.010	20.0±0.3	0.3±0.05
	F:	52.0±3.6	599±68.5	351±30.6	785±54.0	0.0524±0.014	19.0±0.8	0.3±0.06
PND 755	M:	55.0±11.3	505±43.1	183±83.1	609±92.5	0.0325±0.004	14.6±1.2	0.2±0.01
	F:	49.0±18.2	451±98.2	276±17.0	654±69.6	0.0438±0.012	14.3±1.2	0.3±0.1

PND, postnatal day; LL, largest latero-lateral distance of the ventral pouch; VD, the distance between the most ventral point and a line through the alar edge which runs parallel to the tracheal center line; CC, largest rostro-caudal dimension of the ventral pouch; B-Box, bounding box of the thyroid cartilage; VP, ventral pouch.

Figure 1: Size of the ventral pouch (A, ventral view; B, mid-sagittal view). In order to estimate the size of the ventral pouch, three linear distances and its volume were measured. The three measurements were the distance between glottal and alar edge (CC), the largest latero-lateral distance (LL), and the distance between the most ventral point and a line described by CC (VD).

Figure 2: Ventral view and mid-sagittal sections of *Mus musculus* airway at 2 (**A**), 21 (**B**), 90 (**C**), 365 (**D**) and 755 (**E**) days of age. Three-dimensional renditions of the laryngeal airway. The thyroid cartilage is overlaid as transparent object. The ventral pouch (blue) is a small pocket-like expansion from the laryngeal airway which is positioned rostral from the vocal folds (white dashed line) but still inside the laryngeal lumen. The outlines of a box around the thyroid cartilage represent the cartilage's *bounding box* which was used as a proxi for the size of the thyroid cartilage. Note the shape difference of the thyroid cartilage. In pups it demonstrates a narrow cranial opening, but in adults the cranial opening is much wider, divergent (Riede et al. 2020). Black reference bars in lower right corner represent 500 micrometers.

Figure 3 A and B: Three-dimensional laryngeal airway representation of CD1 mice from four age classes (2 day old pups, 21 day old weanlings, 90 day old young adults and 365 day old adults). The ventral pouch is relatively large and sphere-like in pups (A), but increasingly flattens in weanlings (B), young (C) and old (D) adults.

Figure 3C and D: *cont.*

Figure 3E: *cont.*

Figure 4: Size and shape development of the ventral pouch and of the bounding box of the thyroid cartilage throughout the first year of CD1 mice. Measurements were taken in five age classes (2 days; 21 days; 90 days; 365 days, 755 days) from six individuals (3/sex) in each class. **A**, **B** and **C**: Body mass and three linear measures of the ventral pouch. **D**: The thyroid cartilage (described by its bounding box) increases with overall body size. **E**: Ventral pouch (VP) volume does not increase with body mass. **F**: The ratio between the volumes of the bounding box and the ventral pouch decreases with age. **G**: PCA ordinations summarizing major axes of shape variation for the ventral pouch. **H**: Note the almost linear developmental trajectory of the ventral pouch shape. A substantial portion of the shape variation is explained by first principal component (56%).

Figure 5: Mid-organ coronal sections of the larynx of four mice of different ages (in *postnatal days*). In pups, the supraglottal airway, including the ventral pouch fills most of the laryngeal lumen. In older mice laryngeal size increases but the ventral pouch remains rather small. The laryngeal lumen is now filled with soft tissue. The white bar in each image indicates a 0.5 mm distance. Note the dorso-ventral 'flattening' of the thyroid cartilage from PND 365 to 755.

Figure 6: Occurrence of fundamental frequencies in high-frequency whistle calls of three age classes of *Mus musculus*. **A**: Time series and spectrogram of eight inverted-U syllables produced by a female pup. **B**: fundamental frequency was tracked with PRAAT's tracking tool and then exported (**C**). For histogram generation, fundamental frequency was extracted every 5ms and placed in 500 Hz bins. **D**: Fundamental frequency occurrence in syllables from six pups (PND 2), from three young adults (PND 90) and five adults (PND 365) were lumped and plotted in histograms. Fundamental frequency occurrence was quantified by three frequency variables (center F0; minimum and maximum F0). **E**: Strong associations were neither found with body mass nor with ventral pouch (VP) volume. Note that the fundamental frequency range between the three age classes overlap.

Figure 7: Schematic of laryngeal airways shapes in newborn humans (redrawn after Wheeler et al. 2009) and laboratory mice. The pediatric airway was described as conical in shape. The relatively large ventral pouch lumen in the mouse pup, gives its airway a similar wide intra-laryngeal lumen which narrows down into the tracheal airway.

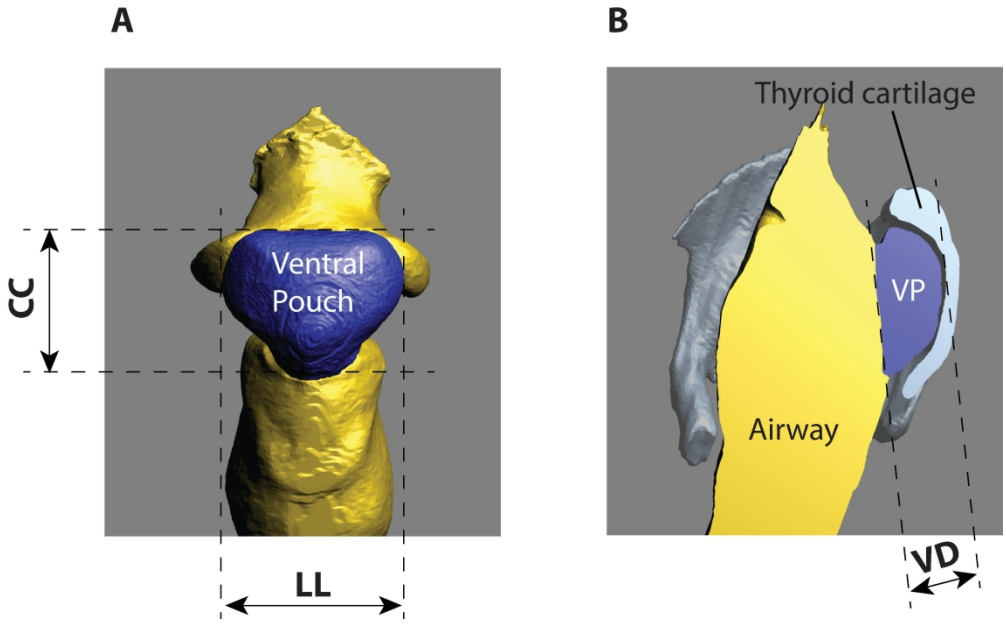

156x96mm (600 x 600 DPI)

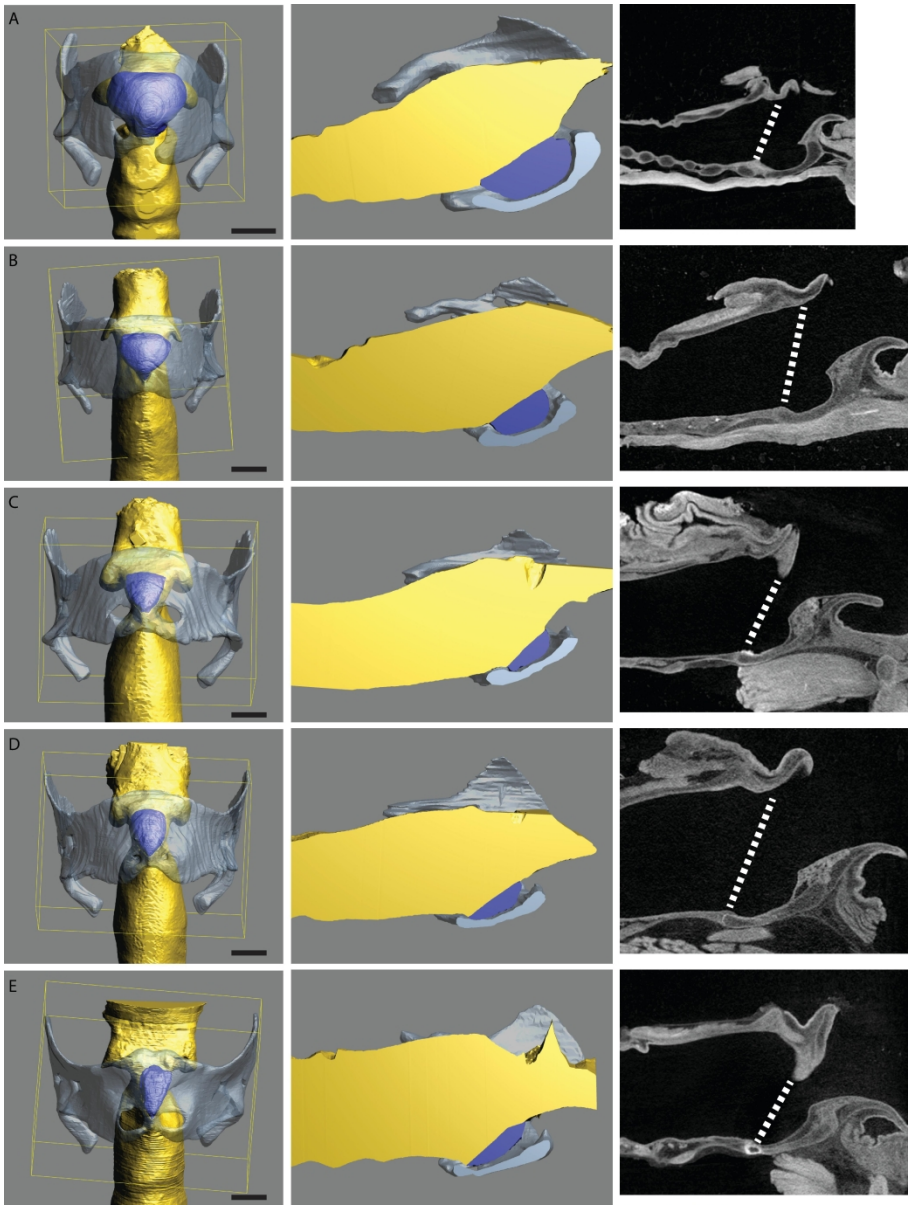

Figure 2

191x253mm (600 x 600 DPI)

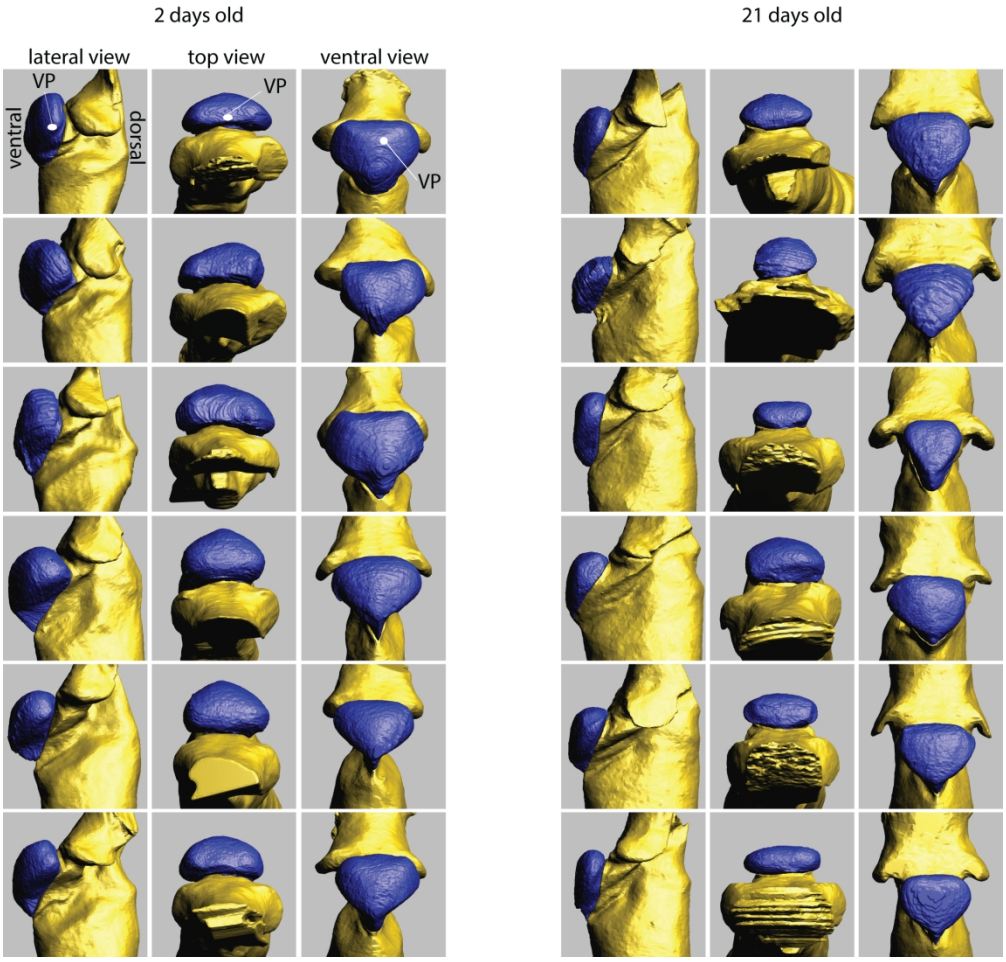
2 days old
21 days old
lateral view
top view
ventral view
VP
VP
VP
ventral
dorsal

Figure 3AB

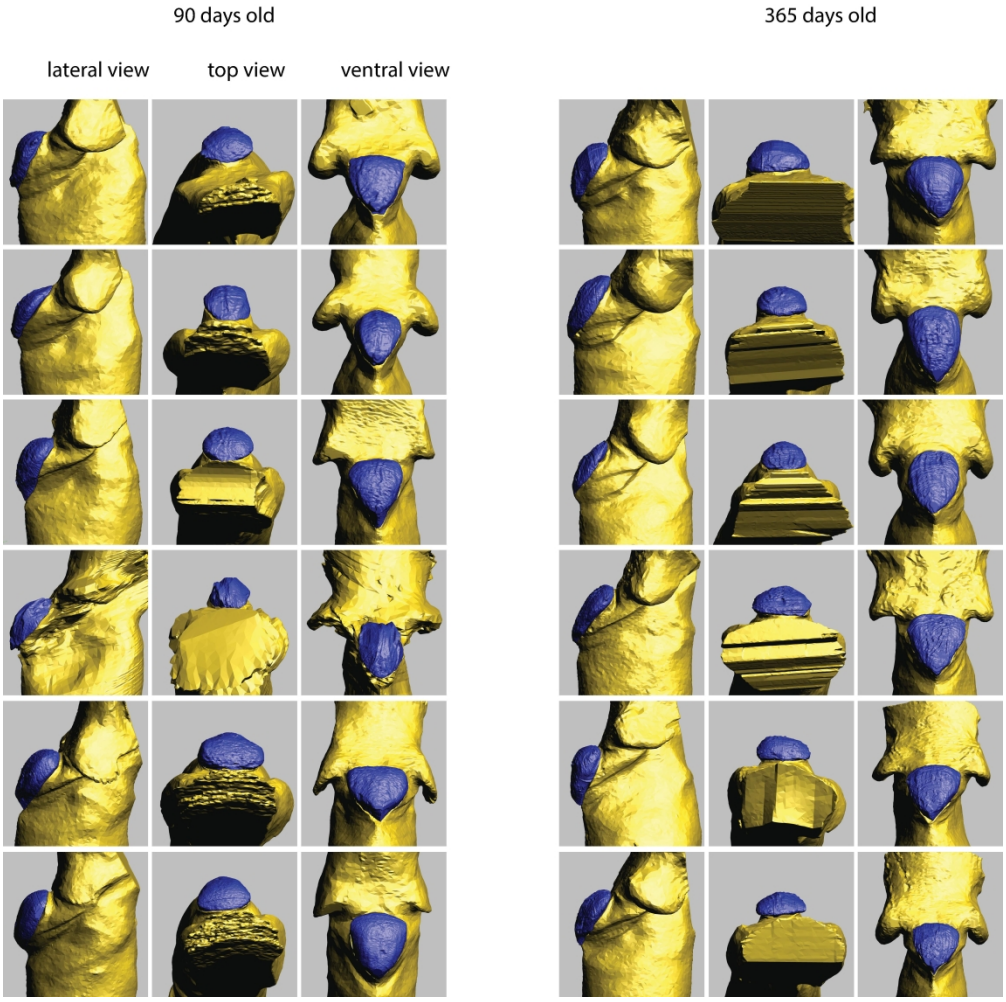

Figure 3CD

195x194mm (600 x 600 DPI)

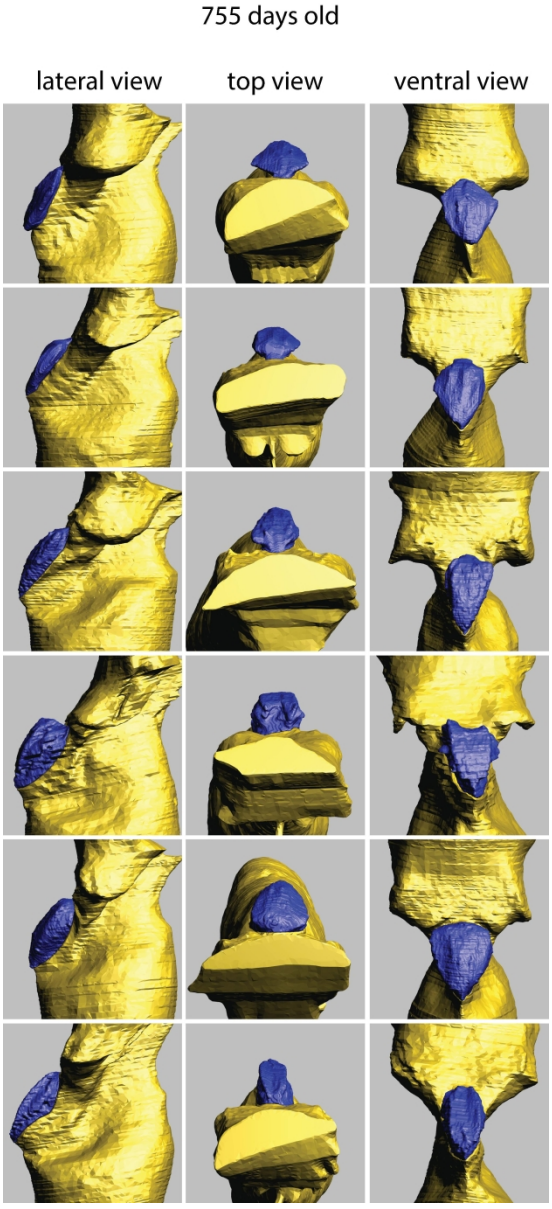

Figure 3E

86x189mm (600 x 600 DPI)

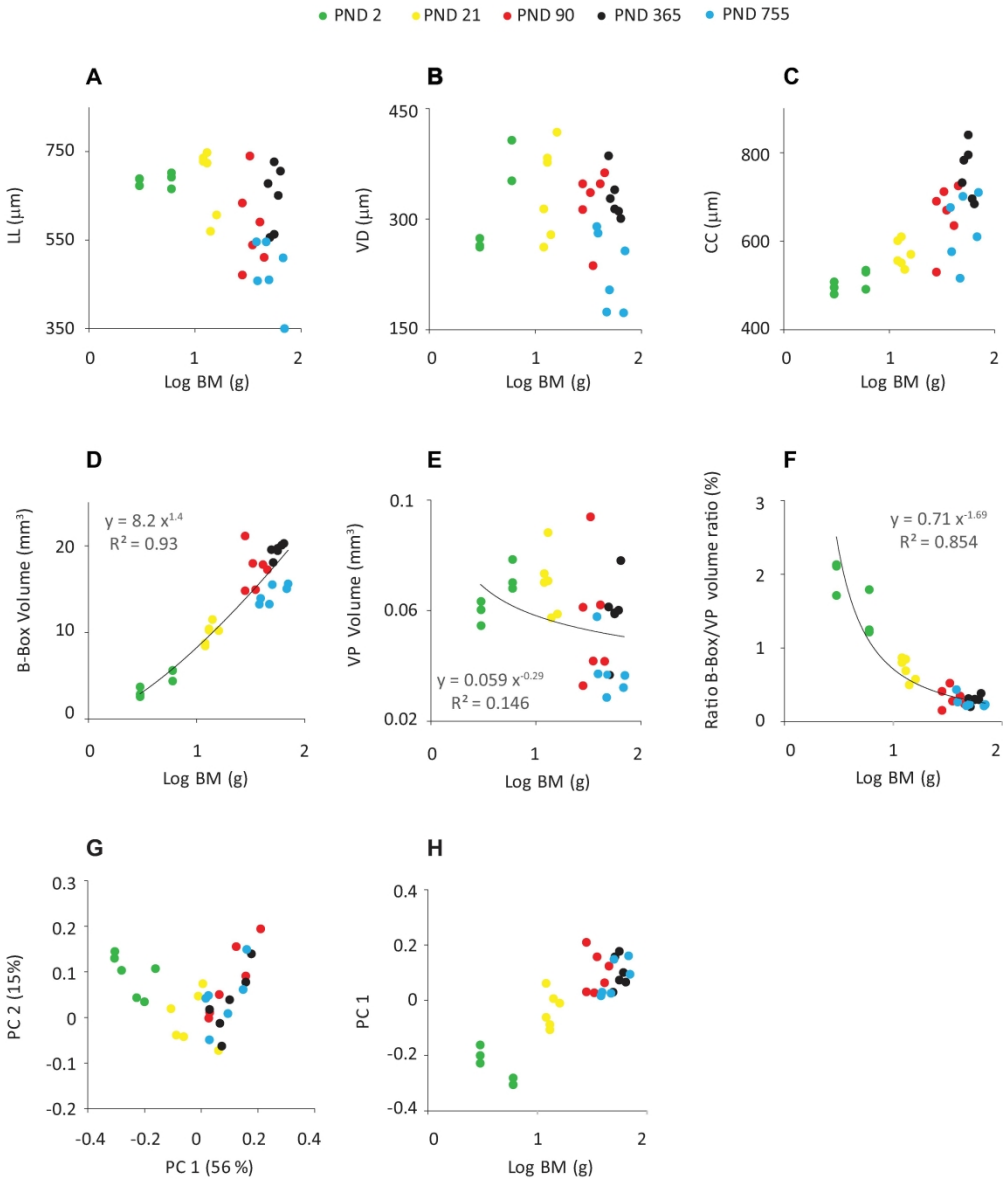

Figure 4

183x215mm (600 x 600 DPI)

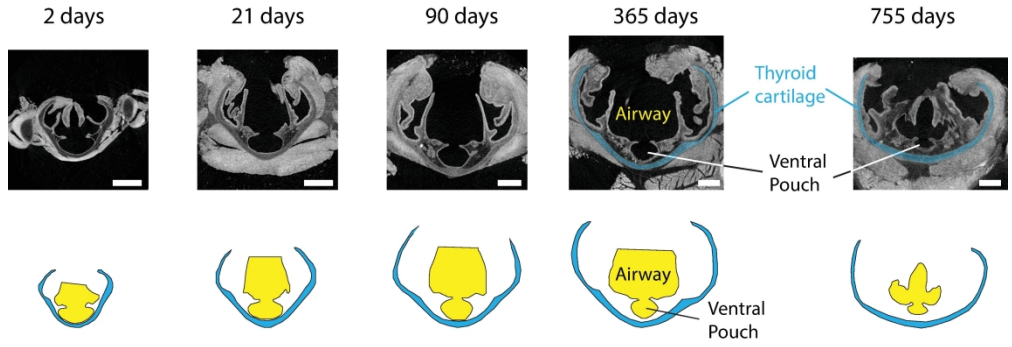

Figure 4

180x61mm (600 x 600 DPI)

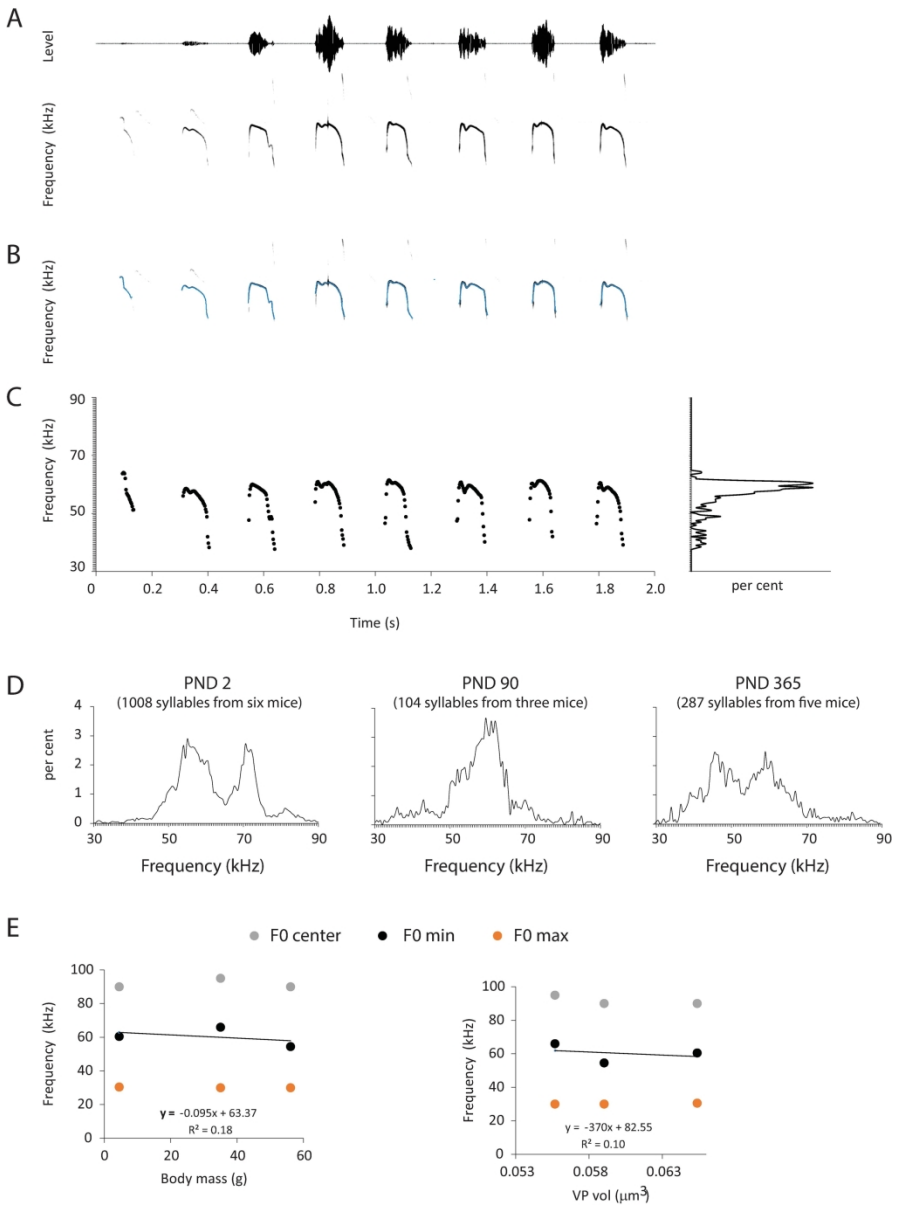

Figure 6

203x275mm (300 x 300 DPI)

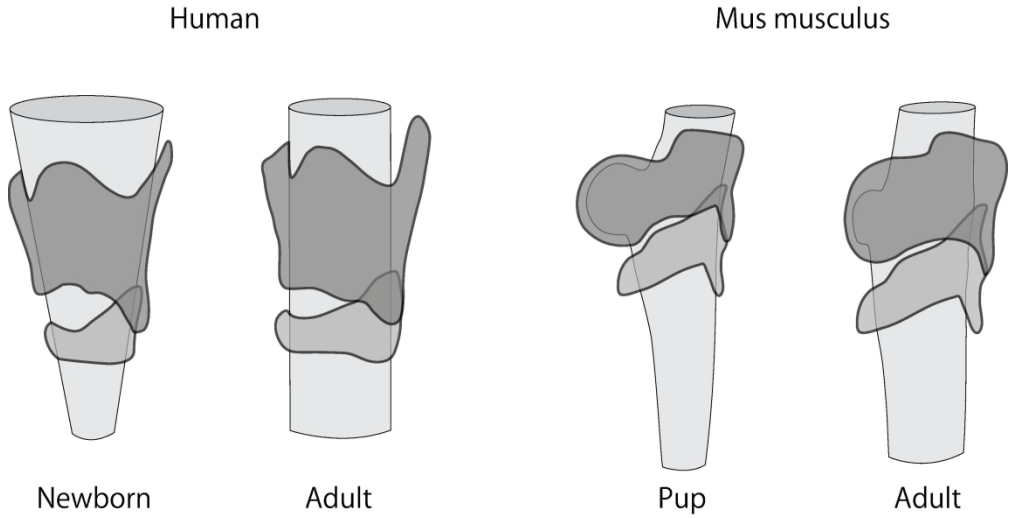

Figure 7

153x78mm (600 x 600 DPI)